

Supplementary data

S1: Detailed description of the Amsterdam Neuropsychological Task (ANT) Battery

(adapted, with permission, from De Sonneville and Lazeron).^{1,2}

Eight tasks from the ANT program were administered to assess speed and accuracy of various tasks. The test stimuli were presented on a computer screen, and the subjects were required to press a mouse key or use the mouse as a tracking device. For patients whose right hand was the dominant hand, the right key was the 'yes' key and the left key the 'no' key; and vice versa for left dominant hand patients. A short description of the tasks used in this study follows.

Baseline Speed

This task measures simple visuomotor reaction time, involving minimal cognitive effort. The subject has to push the 'yes' key whenever a square appears in the center of the screen (see Table 1). The postresponse interval (PRI), the time between response execution and next stimulus onset, is set randomly between 500 and 2500 ms.

Feature Identification

After memorization of a predefined target pattern (see Table 1) subjects have to detect this target pattern in a signal consisting of 4 patterns. Half the signals contain this target pattern (target signals) requiring the subject to press the 'yes'-key, the other half do not (nontarget signals), in which case the 'no'-key should be pressed. For 50% of the target signals the other 3 patterns look very similar to the target, and in the other 50% the other patterns are very dissimilar to the target. Likewise, 50% of the nontarget signals consist of 4 patterns that look similar or dissimilar to the target pattern. The similarity manipulation in this pattern recognition task affects the duration of the encoding stage of processing. The task consists of $4 \times 20 = 80$ trials.

Memory Search Letters

A divided attention (letter detection) task that assesses working memory capacity. It uses a 4-letter display load (see Table 1). The memory load is increased across task parts by increasing the number of letters to be detected in the presented signals from 1 to 3 in part 1, 2 and 3, respectively. The task

parts consists of 40, 72 and 96 trials, respectively, each with 50% target trials ('yes' key) and 50% nontarget trials ('no' key).

Pursuit

This task measures visuomotor control by requiring the participant to continuously track a target moving randomly on the screen (see Table 1). As the trajectory of the target is unpredictable, this task demands the concurrent planning and execution of movements, i.e, executive function. During task performance, the distance between the mouse cursor and the moving target is continuously registered, resulting in 60 distance (deviation) scores.

Tracking

A similar eye-hand coordination task as the pursuit task (see Table S1), but requiring less executive control as the subject has to draw a predefined circle by moving the mouse cursor in between 2 concentric circles. During task performance, the distance between the mouse cursor and the ideal track line is continuously registered, resulting in 60 distance (deviation) scores.

Sustained Attention (Dots)

A continuous performance task, requiring the subject to discriminate between signals containing 3, 4, or 5 dots, presented in 50 series of 12 signals each (see Table 1). The PRI is 250 ms. Fluctuation in speed of processing during time on the task is considered the most important outcome measure.

Shifting Attentional Set (Visual)

This task assesses attentional flexibility, an aspect of executive functioning. A colored square jumps randomly on a horizontal bar to the right or left (see Table 1). Depending on the color of the square right after the jump, the subject has to execute a compatible response (press the key toward where the jump was directed) or an incompatible response ('mirror' movement; press the right key when the jump was to the left and vice versa). This task consists of 3 parts. During the first 2 parts of the task the color is constant (fixed stimulus response mapping), but in the third part the color varies, requiring attentional flexibility by continuously having to adjust response type. The PRI is 250 ms in all parts of the task. The first 2 parts consist of 40 trials, the third part consists of 80 trials.

Visuospatial Sequencing

Memory for visuospatial temporal order (Table 1). In each trial circles are pointed out in a 3x3 matrix of 9 circles. The subject has to point out several circles in the correct temporal order. The number and location of targets varies per trial.

Composite Scores

We defined the composite score for each task depicted in Figure 1D as the average of the relative changes for each component of that task. For example, the Baseline Speed (BS) task measures reaction time (RT) and standard deviation of reaction time (SD).

Hence, BS composite score = $(RT1 - RT0)/RT0 + (SD1 - SD0)/SD0$.

The tests are summarized and depicted graphically in Table S1 below.

Table S1: Amsterdam Neuropsychological Task Battery

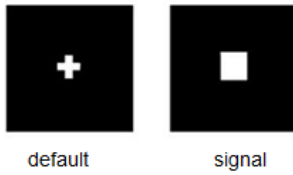
Test	Description	Domain
Baseline Speed	Press 'yes' key when a square appears in the center of the screen.	Simple reaction time, arousal of attention.
Feature Identification	Four patterns are displayed. Decide whether a target pattern is present or not.	Visuospatial memory. Manipulation: degree of similarity between target pattern and distractors.
Memory Search Letters	Four letters are displayed. Decide whether 1 (level 1) or more (level 2 + 3) target letters are present.	Divided attention. Manipulation: memory load, distractors.
Pursuit and Tracking	Pursuit: follow a randomly moving target as closely as possible.	Visuomotor coordination, executive functioning (pursuit > tracking).

	Tracking: draw a circle between predefined boundaries.	
Sustained Attention Dots	Three, 4, or 5 dots are visible on the screen. Press 'yes' for 4 dots; press 'no' for 3 or 5 dots. 50 series of 12 trials each.	Sustained attention (visual).
Shifting Attentional Set	A colored square moves randomly to the right or left. If the square is green, press the key toward where the move was directed; if the square is red, press the key in the opposite direction.	Response organization. Manipulations: inhibition and flexibility.
Visuospatial Sequencing	A matrix of 3x3 circles, of which several are pointed out successively. Repeat this pattern in the correct order.	Visuospatial memory. Manipulation: complexity and relevance of temporal order.

A detailed task description can be found in Supplementary Data 2.

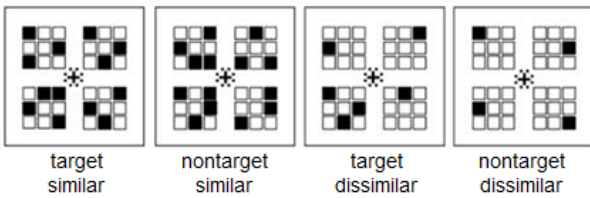
Figure S1 (Continued from Table S1): ANT screen examples

Baseline Speed



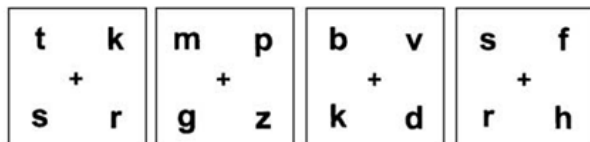
Feature Integration

target =

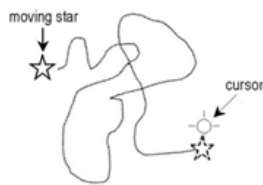


Memory Search Letters

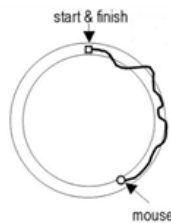
target = k + r + s



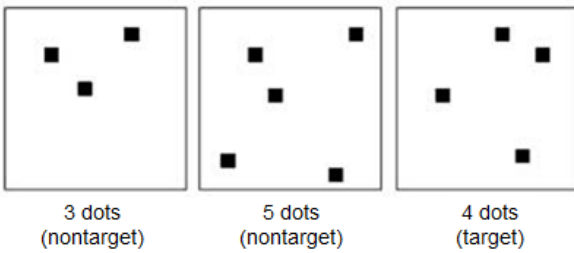
Pursuit



Tracking

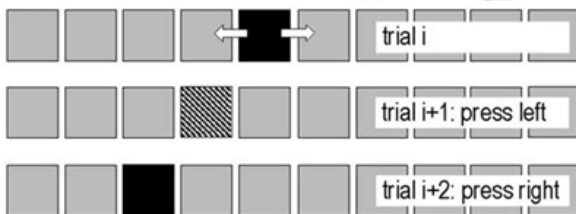


Sustained Attention



Shifting Attentional Set

= green = red



Visuospatial Sequencing

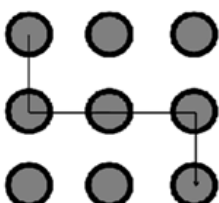


Table S2: MRI Scan Protocol

Scan protocol on 3.0 Tesla MRI (60 minutes)
Sequence Purpose Acquisition Parameters
3D- T1 Volume Sagittal (TI/TR/TE=1000/2730/3.68ms, voxel size 0.8 mm ³)
3D-FLAIR Leukoencephalopathy Axial (TR/TE=11 000/100ms, voxel size 1.1mm ³)
DTI White matter integrity Axial (TR/TE=4800/94, voxel size 2mm ³), 60 slices, 92 directions, b-value 0.1000 s/mm ²
MRS/CSI Metabolite concentrations using 2D Chemical Shift Imaging Axial PRESS (TR/TE=2000/37ms, VOI size 80x80mm, voxel size 10x10x15mm)
ASL Perfusion Pseudo-continuous ASL (TR/TE=4000/14ms, FOV 240x240 mm ² , voxel size 3x3mm ² , slice thickness 7mm, 20 slices, label distance 90mm, label duration 1650ms, postlabeling delay 1525-2281ms)
2D-EPI Resting state fMRI Connectivity (TR/TE=2000/27ms, FOV=240x240mm ² , voxel size 3x3mm ² , 37 slices of 3mm thickness, gap 0.3mm, acquisition duration: 6 minutes)

Image Processing

Image processing included whole brain analysis using Tract Based Spatial Statistics (TBSS) analysis of mean diffusivity (MD) and fractional anisotropy (FA). Our analysis focused on WM tract centers to avoid partial volume effects. All FA-maps were registered to a template, and FA was thresholded at 0.2, creating an FA-skeleton. For each individual subject, its aligned FA and MD maps were projected onto this FA skeleton. Subsequently, FA and MD maps were averaged to a WM summary statistic.^{3,4}

To gain further insight into the origin of diffusion changes, we applied free water imaging as previously described.^{5,6} Briefly, this method uses bitensor modeling to separate the effect from extracellular water and white matter fiber structure on the diffusion signal. Extracellular free water is modeled by an isotropic tensor with fixed diffusion coefficient. After removing the effect of free water, the remaining

diffusion signal is modeled by a free tensor fit, enabling to calculate free water corrected diffusion measures. Because exclusion of CSF partial volume effects is critical in free water imaging, we applied a custom mask as previously described.⁷

T1w, FLAIR and ASL image processing was performed with ExploreASL,⁸ a toolbox that was initiated through the EU-funded COST action "ASL In Dementia"⁹ aiming at harmonizing ASL postprocessing for single-center and multicenter ASL studies. The toolbox is based on Matlab (MathWorks, MA, USA) and Statistical Parametric Mapping 12 (SPM12).¹⁰

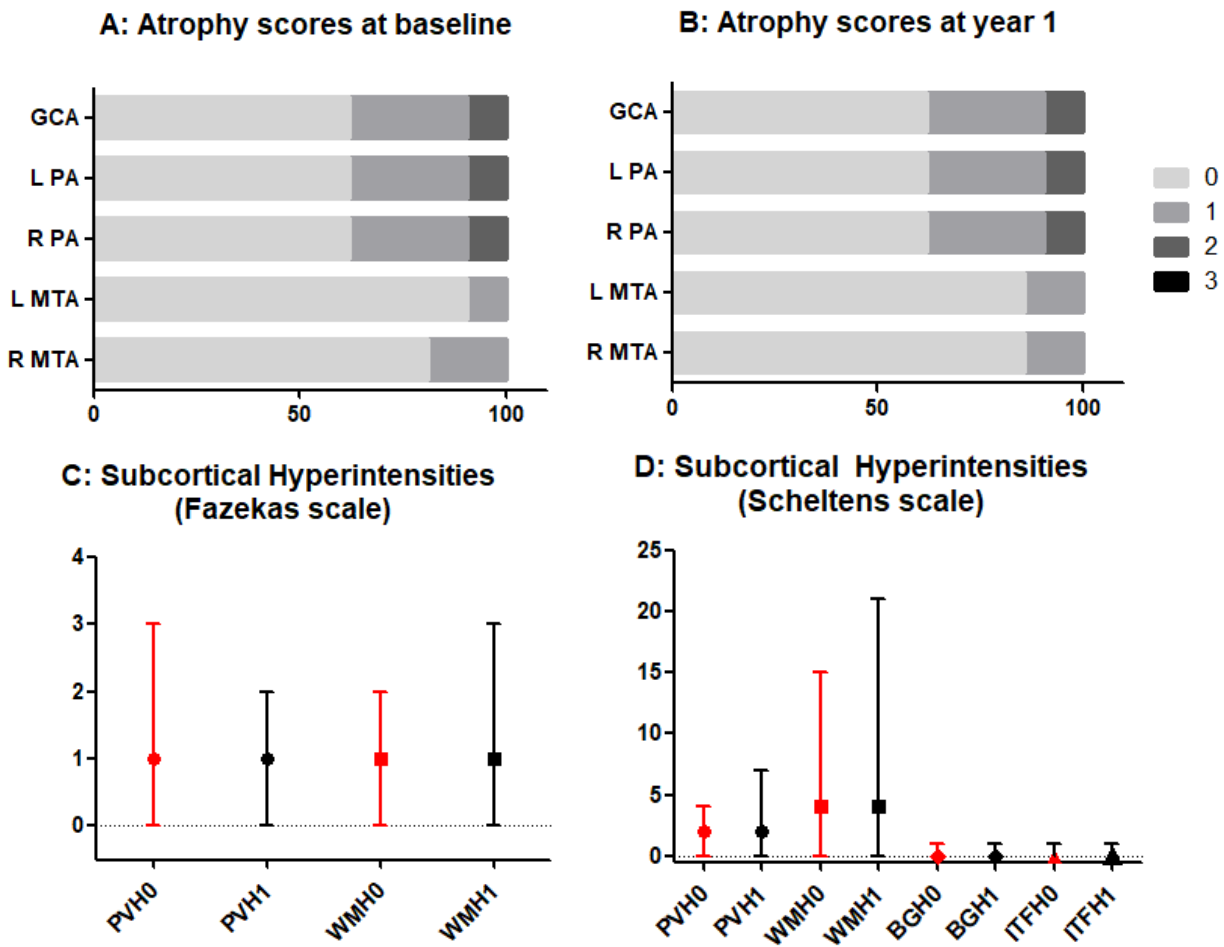
In short, WMH were segmented on the FLAIR images and filled¹¹ on the 3D T1 image using the Lesion Segmentation Toolbox (LST).^{12,13} The 3D T1w images were segmented and registered using the Computation Analysis Toolbox 12 (CAT12)¹⁴ in combination with SPM12 longitudinal registration¹⁵ and Diffeomorphic Anatomical Registration using Exponentiated Lie algebra (DARTEL).¹⁶ Motion correction was performed for ASL datasets using a 3D rigid-body transformation with threshold-free motion outlier exclusion based on a threshold-free optimization of the median GM voxel-wise temporal signal-to-noise ratio (SNR).^{17,18} The M0 images were masked and smoothed, and CBF was quantified using a single compartment quantification model,¹⁹ adjusting for the mean difference in blood T1 due to the mean hematocrit difference before and after transplantation.²⁰ The CBF images were registered to the pGM image.⁸ We analyzed the total GM CBF and spatial CoV.²¹

Metabolite spectra were quantified using tarquin,²² adjusting the phase, estimating the baseline and performing eddy current correction. We excluded spectra with poor signal-to-noise ratios, a disproportionate water signal or other significant artifacts. Based on previous literature, we selected NAA, Cho, Glx as neurometabolites of interest. Metabolite levels were computed as a ratio over Cre, to correct for possibly different contributions of CSF to the voxels of interest (VOIs). Concentrations were subsequently averaged of all VOIs.

RS fMRI data were preprocessed using tools from the FMRIB Software.²³ fMRI time series were visually inspected, brain-extracted, motion-corrected and spatially-smoothed with a 5mm kernel and normalized to MNI space using the T1-weighted image. Subsequently, dual-regression with variance normalization was applied using 10 standard resting state networks⁴ (medial visual, occipital pole, lateral visual areas, default mode, cerebellum, sensorimotor, auditory, executive control, frontal

parietal, frontal parietal) with additional masks for white matter and CSF to regress out residual physiological noise components.²⁴ Statistical analysis were carried out using Randomise (5000 permutations).²⁵ All analyses were initially thresholded at p-value < 0.05 with a family wise error (FWE) correction using threshold free cluster enhancement (TFCE)²⁶ and CBF was added as a confound regressor to the model.

Figure S2: Qualitative MRI Results



A. Atrophy scores at baseline (%); B. Atrophy scores at year 1 (%). C. Subcortical hyperintensities (Fazekas scale, median and range). D. Subcortical hyperintensities (Scheltens scale, median and range). Atrophy and Fazekas scores can range from 0-3; Scheltens scores can range from 0-6 for PVH, from 0-24 for WMH, from 0-30 for BGH, and from 0-24 for ITFH. GCA = global cortical atrophy, PA = posterior atrophy, MTA = medial temporal atrophy, PVH = periventricular hyperintensities, WMH = white matter hyperintensities, BGH = basal ganglia hyperintensities, ITFH = infratentorial foci of hyperintensity.

SUPPLEMENTARY REFERENCES

1. De Sonneville LM, Boringa JB, Reuling IE, et al. Information processing characteristics in subtypes of multiple sclerosis. *Neuropsychologia*. 2002;40(11):1751–1765.
2. Lazeron RH, de Sonneville LM, Scheltens P, et al. Cognitive slowing in multiple sclerosis is strongly associated with brain volume reduction. *Mult Scler*. 2006;12(6):760–768.
3. Smith SM, Jenkinson M, Johansen-Berg H, et al. Tract-based spatial statistics: voxelwise analysis of multi-subject diffusion data. *Neuroimage*. 2006;31(4):1487–1505.
4. Smith SM, Fox PT, Miller KL, et al. Correspondence of the brain's functional architecture during activation and rest. *Proc Natl Acad Sci U S A*. 2009;106(31):13040–13045.
5. Duering M, Finsterwalder S, Baykara E, et al. Free water determines diffusion alterations and clinical status in cerebral small vessel disease. *Alzheimers Dement*. 2018;14(6):764–774.
6. Pasternak O, Sochen N, Gur Y, et al. Free water elimination and mapping from diffusion MRI. *Magn Reson Med*. 2009;62(3):717–730.
7. Baykara E, Gesierich B, Adam R, et al. A novel imaging marker for small vessel disease based on skeletonization of white matter tracts and diffusion histograms. *Ann Neurol*. 2016;80(4):581–592.
8. Mutsaerts HJMM, Petr J, Thomas DL, et al. Comparison of arterial spin labeling registration strategies in the multi-center GENetic frontotemporal dementia initiative (GENFI). *J Magn Reson Imaging*. 2018;47(1):131–140.
9. Arterial spin labeling (ASL) in dementia. 2019. Available at www.aslindementia.org. Accessed June 1, 2018.
10. Ashburner J. SPM: a history. *Neuroimage*. 2012;62(2):791–800.
11. Battaglini M, Jenkinson M, De Stefano N. Evaluating and reducing the impact of white matter lesions on brain volume measurements. *Hum Brain Mapp*. 2012;33(9):2062–2071.
12. Schmidt P, Gaser C, Arsic M, et al. An automated tool for detection of FLAIR-hyperintense white-matter lesions in multiple sclerosis. *Neuroimage*. 2012;59(4):3774–3783.
13. de Sitter A, Steenwijk MD, Ruet A, et al. Performance of five research-domain automated WM lesion segmentation methods in a multi-center MS study. *Neuroimage*. 2017;163:106–114.
14. Structural Brain Mapping Group. CAT: a computational anatomy toolbox for SPM. 2019. Available at <http://www.neuro.uni-jena.de/cat/>. Accessed June 1, 2018.

15. Ashburner J, Ridgway GR. Symmetric diffeomorphic modeling of longitudinal structural MRI. *Front Neurosci.* 2012;6:197.
16. Ashburner J. A fast diffeomorphic image registration algorithm. *Neuroimage.* 2007;38(1):95–113.
17. Wang Z, Aguirre GK, Rao H, et al. Empirical optimization of ASL data analysis using an ASL data processing toolbox: ASLtbx. *Magn Reson Imaging.* 2008;26(2):261–269.
18. Shirzadi Z, Crane DE, Robertson AD, et al. Automated removal of spurious intermediate cerebral blood flow volumes improves image quality among older patients: a clinical arterial spin labeling investigation. *J Magn Reson Imaging.* 2015;42(5):1377–1385.
19. Alsop DC, Detre JA, Golay X, et al. Recommended implementation of arterial spin-labeled perfusion MRI for clinical applications: a consensus of the ISMRM perfusion study group and the European consortium for ASL in dementia. *Magn Reson Med.* 2015;73(1):102–116.
20. Hales PW, Kirkham FJ, Clark CA. A general model to calculate the spin-lattice (T1) relaxation time of blood, accounting for haematocrit, oxygen saturation and magnetic field strength. *J Cereb Blood Flow Metab.* 2016;36(2):370–374.
21. Mutsaerts HJ, Petr J, Václavů L, et al. The spatial coefficient of variation in arterial spin labeling cerebral blood flow images. *J Cereb Blood Flow Metab.* 2017;37(9):3184–3192.
22. Wilson M, Reynolds G, Kauppinen RA, et al. A constrained least-squares approach to the automated quantitation of in vivo ¹H magnetic resonance spectroscopy data. *Magn Reson Med.* 2011;65(1):1–12.
23. Smith SM, Jenkinson M, Woolrich MW, et al. Advances in functional and structural MR image analysis and implementation as FSL. *Neuroimage.* 2004;23(suppl 1):S208–S219.
24. Beckmann CF, Mackay CE, Nicola F, et al. Group comparison of resting-state fMRI data using multi-subject ICA and dual regression. *Neuroimage.* 2009;47(suppl 1):S148.
25. Winkler AM, Ridgway GR, Webster MA, et al. Permutation inference for the general linear model. *Neuroimage.* 2014;92:381–397.
26. Smith SM, Nichols TE. Threshold-free cluster enhancement: addressing problems of smoothing, threshold dependence and localisation in cluster inference. *Neuroimage.* 2009;44(1):83–98.